Forest Canopy Height Mapping in Tanzanian Tropical Rainforests Using Multimodal Remote Sensing Data and Machine Learning

Soheil Zaghian [1,2], Seyed Ehsan Khankeshizadeh [1,2], Sadegh Jamali [1]*, Torbern Tagesson [3], Ernest William Mauya [4], Ali Mohammadzadeh [2], and Filbert Francis [1]

[1] Department of Technology and Society, Faculty of Engineering, Lund University, P.O. Box 118, 221 00 Lund, Sweden. (sadegh.jamali@tft.lth.se; filbert.francis@tft.lth.se)
[2] Department of Photogrammetry and Remote Sensing, Faculty of Geodesy and Geomatics Engineering, K. N. Toosi University of Technology, Tehran 19967-15443, Iran. (soheil.zaghian@email.kntu.ac.ir; seyedehsan.khankeshizadeh@email.kntu.ac.ir; a_mohammadzadeh@kntu.ac.ir)
[3] Department of Earth and Environmental Sciences, Lund University, Sölvegatan 12, Lund, Sweden. (torbern.tagesson@mgeo.lu.se)
[4] Department of Forest Engineering and Wood Sciences, College of Forestry, Wildlife and Tourism, Sokoine University of Agriculture, Morogoro, Tanzania. (mauya@sua.ac.tz)

Keywords: Forest Canopy Height, Machine Learning, GEDI, Random Forest, Gradient Boosting Regression, Remote Sensing.

Abstract

Forest canopy height (FCH) is a critical biophysical parameter that characterizes forest structure and provides fundamental information for estimating above-ground biomass and carbon stocks. The Global Ecosystem Dynamics Investigation (GEDI) Level 2A (L2A) product offers accurate canopy height observations; however, its point-based nature constrains spatial continuity in FCH mapping. This study integrates the multimodal remote sensing datasets for continuous FCH mapping in Tanzania's West Usambara (WUSA) forest, recognized globally for its rich biodiversity and ecological significance. Hence, remote sensing data, including Sentinel-1 polarizations (VV and VH), Sentinel-2 spectral bands and vegetation indices, and the SRTM digital elevation model (DEM), were integrated and matched with GEDI canopy height data used as reference for FCH modelling. The optimal feature set was derived by evaluating the performance of several feature selection and extraction methods, including Principal Component Analysis (PCA), Minimum Noise Fraction (MNF), Recursive Feature Elimination (RFE), Sequential Feature Selection (SFS), and the Selected K-Best approach using F-value and mutual information scoring functions. The feature set derived from RFE, comprising ten features from all data sources, demonstrated the highest accuracy and reliability in FCH modelling. Subsequently, four machine learning algorithms, including Random Forest (RF), Gradient Boosting Regressor (GBR), Support Vector Regressor (SVR), and Ordinary Least Squares (OLS), were evaluated for FCH modelling. Accordingly, RF achieved higher R^2 than GBR, SVR, and OLS, with differences of 0.9%, 8.7%, and 16.4%, respectively. Therefore, the RF model, as the most reliable model, was employed for FCH mapping across the WUSA forest.

1. Introduction

Forest canopy height (FCH) is a fundamental indicator of forest structure, closely associated with above-ground biomass and carbon stocks, serving as a key parameter for climate mitigation monitoring and sustainable forest management (Lei et al., 2024). Remote sensing (RS) provides consistent observations over extensive regions that are difficult to access through ground-based surveys. Airborne Light Detection and Ranging (LiDAR) directly samples vegetation vertical structure and is therefore highly sensitive to canopy height; however, its cost and logistical demands limit repeated wall-to-wall coverage (Hancock et al., 2021). These limitations have been partly alleviated by spaceborne LiDAR missions, such as NASA's Global Ecosystem Dynamics Investigation (GEDI), which provide unprecedented sampling of forest structure (Li et al., 2024). However, the GEDI's point-based measurements lack spatial continuity, underscoring the need for reliable methods to extrapolate canopy height into continuous surfaces.

Therefore, an effective approach is to integrate GEDI footprints with continuous satellite imagery from optical and Synthetic Aperture Radar (SAR) sensors, which together provide complementary information on forest structure (Chen et al., 2025). Although LiDAR systems can directly measure vertical vegetation structure, optical sensors such as Sentinel-2 can be related to canopy chemical and structural properties (Asner and Martin, 2008). However, optical sensors are affected by cloud and haze interference and mainly reflect upper-canopy conditions. In contrast, Sentinel-1 C-band SAR penetrates clouds and is sensitive to canopy moisture and structure, as well as topographic variables that influence terrain-induced radiometric and structural effects (Bruggisser et al., 2021; Cagnina et al., 2023; Pirotti et al., 2023). Previous studies have integrated GEDI relative height (RH) metrics with multimodal datasets to generate FCH maps using machine learning algorithms (e.g., Alvites et al., 2024; Chen et al., 2025), typically employing GEDI as reference samples to learn non-linear relationships for continuous canopy height mapping. Recently, regression models such as k-nearest neighbours, support vector regression (SVR), random forest (RF), and gradient boosting (GB) have been employed for GEDI downscaling because they can handle high-dimensional, non-linear data and provide robust baselines. Furthermore, merely "stacking more layers" does not ensure higher accuracy; modality-aware feature selection or extraction is often necessary to reduce redundancy and enhance transferability across forest types and terrains. For example, Alvites et al. (2024) integrated GEDI, Sentinel-1/2, and topographic data, demonstrating that topography and Sentinel-2 bands were most influential in broadleaf forests, while a combination of SAR, optical, and terrain predictors was more important in coniferous forests.

This contribution has been peer-reviewed. The double-blind peer-review was conducted on the basis of the full paper.
https://doi.org/10.5194/isprs-annals-XI-3-2026-835-2026

They also found that RF and GB outperformed classification and regression trees (CART), and that the choice of RH metric had a significant impact on model performance. More recently, advances in deep learning have demonstrated that learning from image patches can capture spatial textures often overlooked by footprint-based approaches. Lang et al. (2023) trained convolutional neural networks (CNNs) on Sentinel-2 image patches anchored to GEDI footprints to generate canopy height models (CHMs) at a 10 m spatial resolution. Although such models can improve accuracy, they are often data- and computation-intensive. Therefore, well-tuned classical regressors remain attractive for operational mapping when predictors are carefully selected and GEDI shots are quality-controlled (e.g., power-beam selection, sensitivity, and degrade flags). Furthermore, identifying the most effective parameters still requires further investigation due to ecological variability across forest regions, and many previous studies remain valid only within localized contexts.

These considerations are especially salient in tropical mountain systems, such as Tanzania's West Usambara Mountains, where steep terrain, persistent cloud cover, and heterogeneous forest mosaics complicate radiometric normalization and limit the availability of cloud-free optical data. Accordingly, this study proposes a pragmatic and information-efficient integration of Sentinel-1 VV/VH backscatter, Sentinel-2 spectral bands and indices, and SRTM-derived terrain variables, calibrated against screened GEDI L2A RH metrics, to provide a robust framework for dense FCH mapping in heterogeneous topography. Therefore, the main contributions of this study are highlighted as follows:

1. Mapping FCH using a multimodal remote sensing dataset (Sentinel-1, Sentinel-2, SRTM, and GEDI L2A).
2. Comparing the performance of machine learning algorithms for FCH modelling (Random Forest, SVR, Gradient Boosting Regressors, and Ordinary Least Squares).
3. Evaluating the contribution of various features and identifying the optimal feature set for FCH modelling.
4. Producing wall-to-wall FCH maps for the tropical mountainous forests of the WUSA region.

2. Study Area and Data

2.1. Study Area

The present study focuses on FCH mapping in the West Usambara (WUSA) Mountains, located in the Tanga Region of northern Tanzania (Figure 1). This region is part of the Eastern Arc Mountains, a series of ancient and isolated mountain blocks stretching from south-eastern Kenya to south-central Tanzania. The West Usambara block spans approximately 2,200 km² and exhibits a substantial altitudinal gradient, extending from about 400 m to over 2,200 m above sea level. The landscape is characterized by heterogeneous topography comprising steep escarpments, deeply incised valleys, and undulating ridges, which sustain vegetation ranging from lowland and sub-montane to high-elevation evergreen forests. Notable forest reserves within this region include Magamba Nature Forest Reserve, Shagayu, Ndelemai, and Balangai, which host a rich assemblage of characteristic Eastern Arc tree species such as Newtonia buchananii, Parinari excelsa, Albizia gummifera, Ocotea usambarensis, and Allanblackia stuhlmannii (Mauya & Madundo, 2021). The West Usambara Mountains are recognized as a global biodiversity hotspot due to their high endemism and ecological significance, providing essential ecosystem services such as water regulation. Their unique ecology, conservation value, and varied management regimes make them an ideal setting for studying environmental dynamics in complex tropical montane forests.

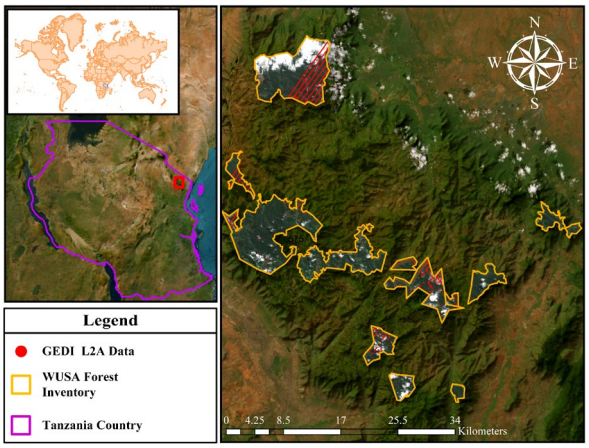

Figure 1. The Study Area in the West Usambara (WUSA) Mountains is located in northern Tanzania.

2.2. Data

This study leverages the multimodal RS imagery and GEDI-L2A dataset to generate continuous canopy height mapping. Table 1 summarizes all of the satellite RS datasets that were employed in this study for FCH mapping.

Satellite	Utilized features	Feature	Description
Sentinel -1	Polarization	VV	-
		VH	
Sentinel -2	Spectral Bands	B1	Aerosols [443 nm]
		B2	Blue [490 nm]
		B3	Green [560 nm]
		B4	Red [665 nm]
		B5	Red Edge 1 [705 nm]
		B6	Red Edge 2 [749 nm]
		B7	Red Edge 3 [783 nm]
		B8	NIR1 [842 nm]
		B8A	NIR2 [865 nm]
		B9	Water vapor [945nm]
		B11	SWIR1 [1610 nm]
		B12	SWIR2 [2190 nm]
	Spectral Indices	NDVI	(NIR - Red) / (NIR + Red)
		MNDWI	(Green - SWIR)/ (Green + SWIR)
		NDMI	(NIR - SWIR1) / (NIR + SWIR1)
		NDRE	(NIR - Red edge) / (NIR + Red edge)
		EVI	2.5 × ((NIR - RED) / (NIR + 6 × RED - 7.5 × BLUE + 1))
SRTM	Elevation Data	DEM	-
GEDI	Elevation Data	Canopy Top Height	Relative heights at 98%

Table 1. Summary of the datasets utilized for FCH modelling.

This contribution has been peer-reviewed. The double-blind peer-review was conducted on the basis of the full paper.
https://doi.org/10.5194/isprs-annals-XI-3-2026-835-2026 | © Author(s) 2026. CC BY 4.0 License.

2.2.1. GEDI (L2A): The GEDI Level 2A (L2A) product was used as the reference dataset for estimating forest canopy height. GEDI provides high-resolution lidar measurements of Earth's three-dimensional vegetation structure between 51.6° N and 51.6° S, offering one of the densest global samples of canopy height. The Level-2A (L2A) product consists of rasterized canopy height estimates at 25 m spatial resolution derived from 100 Relative Height (RH) metrics, which collectively represent the full waveform profile of each lidar shot (Li et al., 2023). In this study, monthly composite GEDI L2A scenes were obtained from the Google Earth Engine (GEE) catalogue ("LARSE/GEDI/GEDI02_A_002_MONTHLY"), which includes 136 bands containing RH metrics, quality flags, and associated metadata.

2.2.2. Sentinel-1: Sentinel-1 is a C-band SAR sensor that captures all-weather SAR data in two polarization modes of VH and VV. Here, the Ground Range Detected (GRD) products captured in the Interferometric Wide-Swath mode with 10-meter spatial resolution, available in the GEE data catalog ("COPERNICUS/S1_GRD"), were employed (Ghorbanian et al., 2025). These data underwent initial preprocessing steps (e.g., radiometric calibration and terrain correction). A monthly composite of this satellite image from 2024 was generated to synchronize the data collection with the GEDI data.

2.2.3. Sentinel-2: Sentinel-2 carries the Multi-Spectral Imager (MSI), which images the Earth's surface in 12 bands with different spatial resolutions ranging between 10 and 60 m. Here, Level-2A Sentinel-2 harmonized surface reflectance data, available in the GEE data catalogue ("COPERNICUS/S2_SR_HARMONIZED"), were employed. These data were initially pre-processed using the Sen2Cor framework that applies atmospheric, terrain, and cirrus corrections to generate surface reflectance data (Ghorbanian et al., 2025). To synchronize the data collection with GEDI, monthly composites from 2024 were generated based on a 5% percent cloud-cover threshold. Finally, all of the available surface spectral reflectance bands and some of the spectral indices were collected to model the FCH (See Table 1).

2.2.4. DEM (SRTM): The Shuttle Radar Topography Mission (SRTM) digital elevation model (DEM), produced by NASA's 2000 mission (Farr et al., 2007), was used to incorporate terrain-related variables into the FCH modelling. The SRTM Version 3 (SRTM Plus) dataset provides near-global elevation coverage at a spatial resolution of 1 arc-second. It remains one of the most reliable DEM sources, particularly in forested regions where it effectively captures canopy–ground separation. In this study, the SRTM DEM was obtained from the GEE catalogue ("USGS/SRTMGL1_003") to represent topographic variability consistently across the study area.

3. Methodology

Figure 2 illustrates the flowchart of the proposed framework for selecting the optimal feature collection and subsequently modelling FCH, as well as continuous canopy height mapping through the integration of multimodal RS datasets. Hence, this section is divided into three main subsections: 1) pre-processing for preparing the matched dataset, 2) Feature selection, and 3) FCH modelling and mapping.

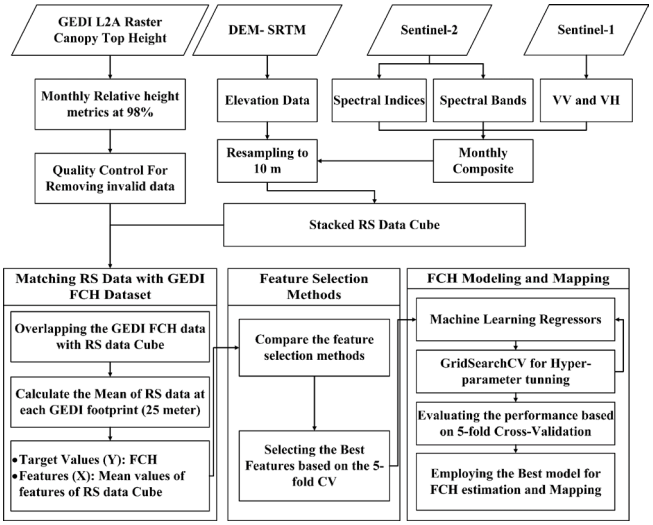

Figure 2. Flowchart of the proposed methodology for generating a continuous FCH mapping from GEDI data and multi-source RS imagery.

3.1. Pre-processing and Data Preparation

At the first stage, to minimize potential noise in the upper canopy returns (i.e., rh100), the 98th percentile relative height (rh98) was extracted from the GEDI L2A raster canopy dataset (Li et al., 2023; Rajab Pourrahmati et al., 2023). This metric represents laser returns near the top of the canopy and was used to characterize canopy height. As illustrated in Figure 2, quality control was implemented to remove the invalid records from the GEDI waveform dataset. The "quality flag" attribute was used to exclude invalid GEDI data with a value of 0. Consequently, pure high-quality canopy heights were collected over the WUSA forest inventory for all months of 2024, as the target values for FCH modelling and mapping.

Furthermore, the monthly composites of Sentinel-1 and Sentinel-2 images were generated to synchronize the satellite imagery with the GEDI dataset. Notably, all Sentinel-2 scenes with cloud cover exceeding 5% were excluded, and monthly composites were generated using the median values of the remaining images in each month. Moreover, several spectral indices were computed, including Normalized Difference Vegetation Index (NDVI), Modified Normalized Difference Water Index (MNDWI), Normalized Difference Moisture Index (NDMI), Normalized Difference Red Edge Index (NDRE), and Enhanced Vegetation Index (EVI) (See Table 1).

Finally, all features, including monthly composites of polarizations, spectral reflectance bands, spectral indices, and DEM, were concatenated to generate the RS data cube serving as independent variables for FCH modelling. In addition, all features in the RS data cube were resampled to a 10 m resolution using the nearest-neighbour algorithm to ensure spatial alignment. Finally, all GEDI raster canopy height footprints were overlaid onto the RS data cube (Figure 3). Since the pixel resolution of GEDI images is 25m, each pixel of this data encompasses several pixels in the RS data cube. The mean values of the RS pixels within each GEDI footprint were therefore calculated to serve as the independent variables, resulting in 1478 samples with averaged RS feature values paired with their corresponding canopy height measurements.

This contribution has been peer-reviewed. The double-blind peer-review was conducted on the basis of the full paper.
https://doi.org/10.5194/isprs-annals-XI-3-2026-835-2026 | © Author(s) 2026. CC BY 4.0 License.

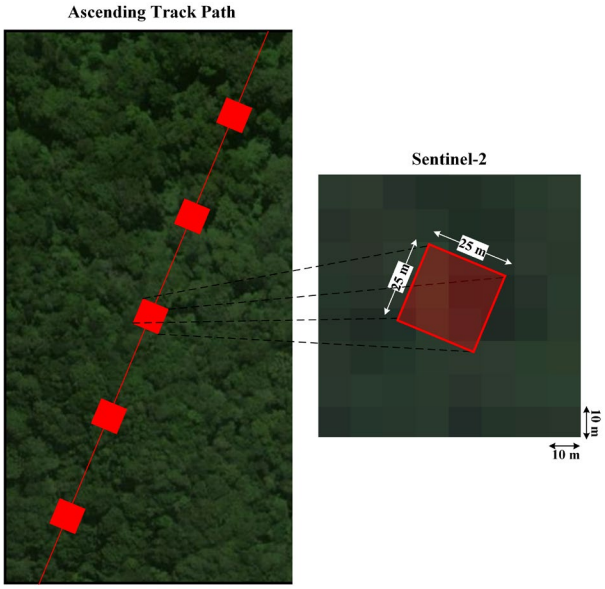

Figure 3. Footprint of laser beams on the ascending track path overlapped on the Sentinel-2 imagery to match up the dataset and extract the samples.

3.2. Feature Selection

A total of 20 different features were collected for FCH mapping (Table 1). Two feature extraction and four feature selection methods were selected for the FCH modelling. The feature extraction methods, including Principal Component Analysis (PCA) and Noise Minimum Fraction (NMF), were applied to derive a new feature collection. The feature extraction methods transform the feature collection into a new feature set by using fundamental statistical criteria. Furthermore, feature selection methods, including Recursive Feature Elimination (RFE), Sequential Feature Selector (SFS), Selected k-best with two scoring functions (i.e., F-value and Mutual information), were applied to identify the optimal feature set. Accordingly, all possible feature combinations were generated using the mentioned method, and the feature set yielding the best performance was selected as the optimal feature set for FCH modelling. Notably, the RF regression model was employed in this section to evaluate the performance of the feature collections and identify the most important features. The optimal feature collection was selected based on accuracy from a 5-fold cross-validation, ensuring that the chosen features maximize predictive performance while minimizing redundancy.

3.3. FCH Modelling and Mapping

The FCH modelling was performed using the optimal feature collection, which comprised pure and qualified samples derived from the previous section. Accordingly, four different machine learning regression models, including Random Forest (RF), Support Vector Regressor (SVR), Gradient Boosting Regressor (GBR), and Ordinary Least Squares (OLS), were applied to predict FCH.

To optimize the performance of each regression model, the Grid Search Cross-Validation (CV) was employed for hyper-parameter tuning. Table 2 indicates the parameters of each machine learning model used in the Grid Search CV to achieve optimal performance. The total number of trained models was determined by the combinations of hyperparameters and folds in the dataset. The best-performing model was then selected for FCH modelling and mapping across the WUSA forests.

ML model	Parameters	values	N. models
RF	Number of trees	50, 100, 200, 300, 500, 600, 700, 800, 900, 1000	1080
	Tree Depth	None, 10, 20, 30	
	Min Samples split	2, 5, 10	
	Min samples leaf	1, 2, 4	
	Max feature	5, 10, 20	
GBR	Number of estimators	100, 200, 300, 500, 600, 700, 800, 900, 1000	810
	Max depth	3, 4, 5	
	Learning Rate	0.001, 0.01, 0.05, 0.1, 0.2	
	Subsample	0.8, 1.0	
	Max Feature	5, 10, 20	
SVR	Kernel	Polynomial, RBF, sigmoid, linear	896
	C	0.001, 0.01, 0.1, 10, 100, 1000, 10000	
	Gamma	Scale, auto	
	epsilon	0.01, 0.1, 0.5, 1	
	degree	2, 3, 4, 5	
OLS	-		1

Table 2. Summary of parameters evaluated in machine learning algorithms to find the optimal model.

Moreover, a 5-fold cross-validation approach was conducted to evaluate the performance of machine learning models in FCH estimating. Accordingly, each sample served as a test case once, allowing model performance to be assessed across the entire dataset. As a result, the optimal model leverages higher generalizability with minimal data dependency. Hence, four statistical criteria, including the Coefficient of determination (R^2), Root Mean Square Error (RMSE), Mean Absolute Error (MAE), and Mean Absolute Percentage Error (MAPE), were calculated in the accuracy assessment using the 5-fold CV approach, as follows:

$$R^2 = 1 - \frac{\sum_{i=1}^{n}(y_i - \hat{y}_i)^2}{\sum_{i=1}^{n}(y_i - \bar{y})^2}, \quad (1)$$

$$RMSE = \sqrt{\frac{1}{n}\sum_{i=1}^{n}(y_i - \hat{y}_i)^2}, \quad (2)$$

$$MAE = \frac{1}{n}\sum_{i=1}^{n}|y_i - \hat{y}_i|, \quad (3)$$

$$MAPE = \frac{1}{n}\sum_{i=1}^{n}\left|\frac{y_i - \hat{y}_i}{y_i}\right| \times 100, \quad (4)$$

where n = number of samples

$\hat{y}_i$ = Predicted value of the ith sample

y_i = Actual value of the ith sample

$\bar{y}$ = Mean of predicted values

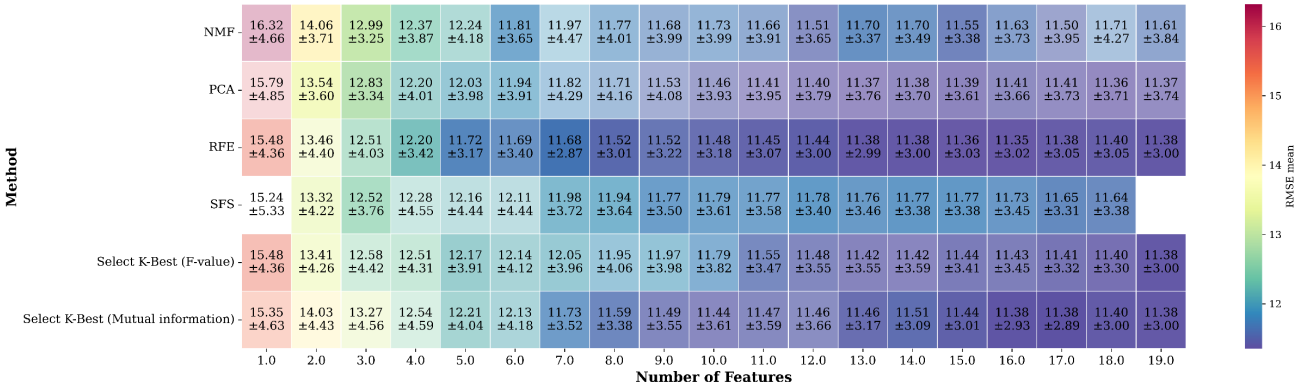

Figure 4. Heat map of feature selection results, based on the RMSE values. The colour of the heatmap indicates the mean of the RMSE values, and the variance of RMSE is depicted by the transparency.

4. Results

4.1. Feature Selection

Figure 4 presents the accuracy of each feature collection, categorized by feature selection/extraction method, with respect to feature count. For each cell, the mean RMSE with associated variance from 5-fold CV is shown; darker, more saturated colours indicate lower mean RMSE and smaller variance, reflecting better and more stable performance. Conversely, lighter and warmer colours correspond to higher mean RMSE and larger variance, signalling poorer accuracy and greater uncertainty in model predictions. The PCA outperformed the NMF, the other feature extraction method, demonstrating both higher accuracy and greater stability. However, except for the SFS method, which indicated the lowest performance in this study, all other feature selection methods performed comparably to PCA. Accordingly, RFE and Select K-Best (using both F-value and Mutual Information) demonstrated strong performance in selecting features for FCH modelling. In general, the RFE, PCA, and selected k-best (based on mutual information) methods indicated the best performance based on the mean RMSE values, and their performances are significantly close to each other. However, the RFE exhibited the lowest variance in RMSE values, indicating the most reliable performance in selecting the feature collection for FCH modelling. In this method, selecting 8-13 features mitigated the RMSE variance and significantly reduced uncertainty compared to other collections. As a result, a 10-feature collection with an RMSE of 10.87 ± 1.27 was selected as the most reliable feature collection for FCH mapping.

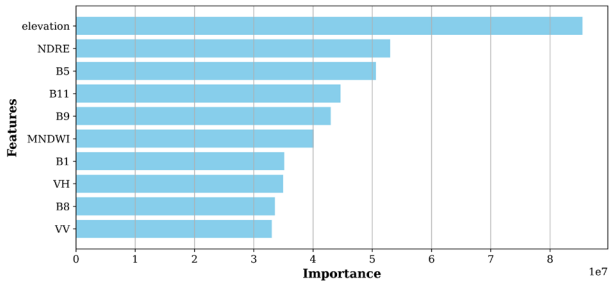

Figure 5. The feature importance of the selected feature collection from the RFE method for FCH modelling.

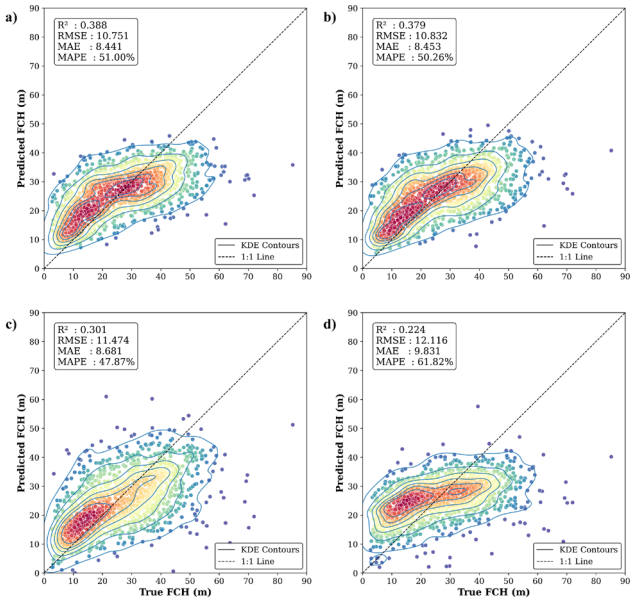

Figure 6. Scatter plots showing the results of FCH modelling based on a) RF, b) GBR, c) SVR, and d) OLS.

Although this set did not have the lowest mean RMSE, considering both the mean and variance, it demonstrated the most reliable performance. Figure 5 presents the feature importance of the selected RFE-derived feature collection (i.e., with 10 features), which was subsequently employed in the RF regression model for FCH estimation. Notably, the elevation variable obtained from the SRTM DEM exhibited a strong influence on FCH modelling, which is consistent with the intrinsic relationship between canopy height and elevation characteristics. Furthermore, the selected feature collection integrates all feature categories, including spectral reflectance bands (e.g., B11, B9, B8, and B1), spectral indices (e.g., NDRE and MNDWI), and SAR polarization components (e.g., VH and VV). Accordingly, the combination of diverse features underscores their critical role in FCH modelling, highlighting the importance of integrating multimodal datasets for accurate FCH estimation and mapping. Accordingly, the RFE-derived feature collection comprising ten selected features was employed for the comparative evaluation of regression models and for FCH mapping in the subsequent sections.

This contribution has been peer-reviewed. The double-blind peer-review was conducted on the basis of the full paper.
https://doi.org/10.5194/isprs-annals-XI-3-2026-835-2026 | © Author(s) 2026. CC BY 4.0 License.

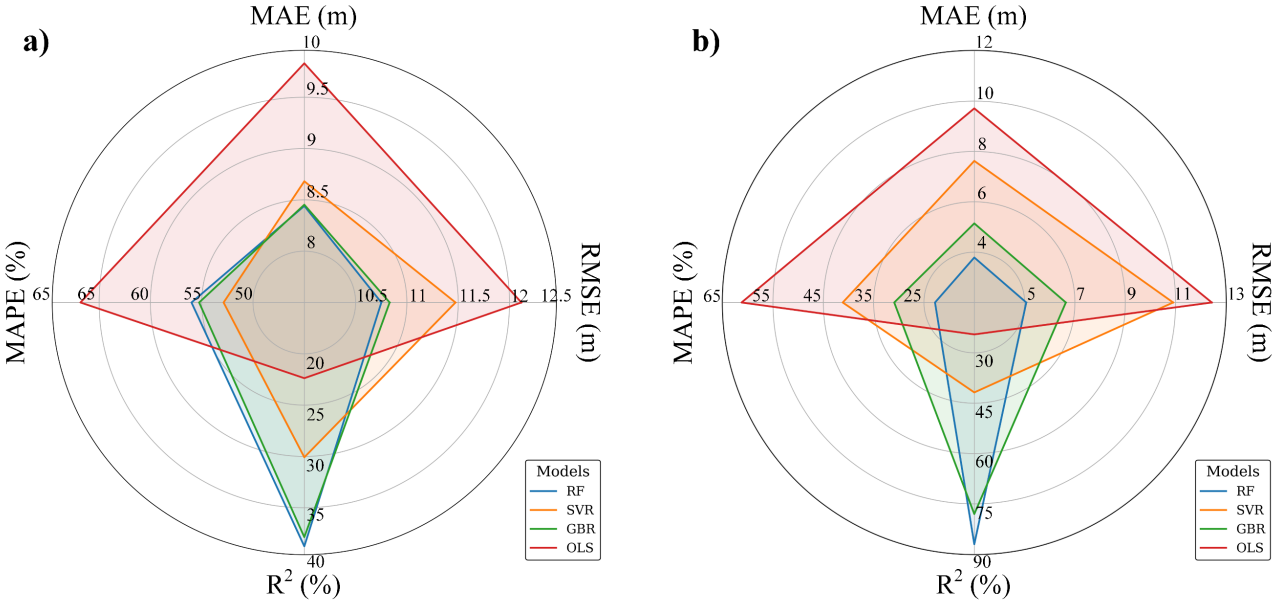

Figure 7. Performance of the machine learning models in FCH estimation for a) Test, and b) Train samples. Model performance is evaluated using R^2 (%), MAE (m), RMSE (m), and MAPE (%). Higher R^2 values indicate better model performance, whereas lower MAE, RMSE, and MAPE values represent lower prediction errors and therefore better accuracy.

4.2. FCH Modelling

Figure 6 compares the performance of regression models, including RF, GBR, SVR, and OLS, in predicting FCH values. Results are aggregated from a 5-fold CV approach, with each fold serving once as the test set; thereby, the figure summarizes model performance across all samples. Although the RMSE and R^2 values differ substantially between the two ensemble models (i.e., RF and GBR) and the SVR and OLS models, the differences in MAE values are comparatively minor (Figure 6). Furthermore, unlike the other accuracy metrics, the MAPE values exhibit a distinct pattern. Accordingly, SVR achieved the lowest MAPE, which was 2.39% and 3.13% lower than the MAPE values of GBR and RF, respectively. While RMSE emphasizes larger prediction errors, MAPE scales each error by the true value to highlight relative error, and MAE reflects the overall average error. Therefore, the RF and GBR demonstrated more reliable performance in predicting the FCH values (see Figure 6a and b) compared with SVM (Figure 6c), particularly as they maintain lower errors across a wider range of canopy heights. Furthermore, the OLS exhibited the poorest performance in predicting FCH values (see Figure 6d), showing substantial errors across the entire range of canopy heights. This fact suggests that predicting FCH values is a complex problem that OLS struggles to handle effectively. Although the performance of the RF and GBR was significantly similar, the RF slightly outperformed the GBR, particularly for the higher FCH values. In general, the RF model indicated a more reliable and generalized performance.

Moreover, Figure 7 indicates the performance of the machine learning models for both predicting test samples and the training stage. Figure 7a illustrates that RF and GBR exhibited very similar performance in predicting the test FCH samples. Furthermore, these two models (i.e., RF and GBR) outperformed the other machine learning models (i.e., SVR and OLS) in predicting FCH in this study. Moreover, OLS exhibited the weakest performance among the models for predicting the test samples, indicating that FCH modelling requires a more complex approach. The results also confirm that RF slightly outperformed GBR. In addition, Figure 7b reveals that the RF model achieved remarkably higher performance in fitting the training samples. Although RF and GBR performed similarly in predicting the samples, RF demonstrated significantly higher performance during training. This suggests a potential overfitting in the RF model, indicated by the substantial difference between its training and test predictions. However, the high training accuracy indicates that the machine learning models were able to fit the training samples effectively. Hence, the remarkable decrease in predicting unseen samples underscores the challenge of FCH. As shown in Figure 7b, SVR and OLS exhibit significantly lower training accuracy compared with RF and GBR, indicating that these models suffer from underfitting, which reduces their predictive accuracy. The RF demonstrated more reliable and superior performance in both training and test sample predictions.

The results indicated performance compatible with the previous studies on FCH estimation. The present results concur with those of Alvites et al. (2024), in which GEDI, Sentinel-1/2, and topographic predictors were integrated and used to train RF, CART, and GB regressors for forest canopy height (FCH) estimation. Similarly, the RF and GB outperformed other machine-learning models, reinforcing the effectiveness of ensemble learners for canopy-height estimation. These findings are consistent with those of the present study, where topography and Sentinel-2 spectral bands likewise emerged as dominant predictors in broadleaf forest environments. Furthermore, the results of this study are broadly consistent with those reported by Chou et al. (2024), who used Sentinel-1, Sentinel-2, spectral indices, terrain predictors, and GEDI (rh99) as the reference for canopy-height estimation. In their study, a CNN was trained to predict GEDI (rh99) in southeastern Australian forests, and an RMSE of 10.1 m was reported. In a comparable study, Pourshamsi et al. (2021) combined polarimetric SAR (PolSAR) variables with LiDAR-derived FCH measurements and evaluated RF, SVM, Rotation Forest, and Canonical Correlation

Forest models. An average RMSE of 10 m was reported across algorithms and training samples, which is comparable to the RMSE obtained by the RF model trained on the RFE-derived feature set in the present study. Moreover, a major source of uncertainty in FCH estimation in this study was the heterogeneous topography of the mountainous WUSA forest. Li et al. (2024) reported that GEDI-based FCH estimates are strongly influenced by canopy cover, forest type, and terrain slope, with RMSE increasing to as much as 13.26 m under adverse conditions.

4.3. FCH Mapping

The trained RF model using the identified optimal feature collection was applied to the RS data for FCH mapping across the conservation regions of the WUSA forest inventory (Figure 8). The FCH map is provided based on the monthly Earth observation data from November 2024. Hence, the high-resolution FCH map (i.e., 10m) captures the wide variation in canopy height, ranging from 8 to 46 m across the forested areas. Accordingly, the regions with higher canopy height (shown in green to blue) are predominantly located in the southern and eastern regions, and sparsely in the central part of the forest. Conversely, the regions with the lower canopy height (indicated in yellow to red) are significantly concentrated in the western and north-western parts of the study area. This heterogeneity reflects variations in forest structure and underscores the ecological and biodiversity significance of these regions across the landscape.

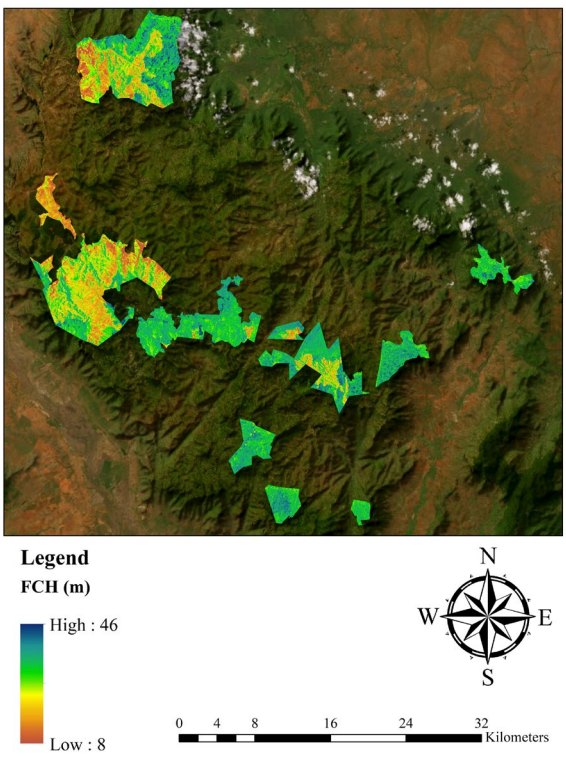

Figure 8. FCH map of the WUSA forest.

5. Conclusion

The present study focused on integrating multimodal RS datasets to estimate continuous canopy height. In the first stage, the performance of feature extraction and selection methods was evaluated to identify the optimal feature set. The optimal set was ultimately obtained using the RFE method and included all feature types—DEM, spectral bands, spectral indices, and SAR polarizations—highlighting the importance of multimodal RS datasets for FCH modelling. Subsequently, the selected features were used to compare the performance of different machine learning regression algorithms. Random Forest was identified as the best-performing model for wall-to-wall FCH mapping across the mountainous tropical rainforest of the WUSA forest. In conclusion, the monthly FCH maps produced in this study can support forest management and serve as a basis for estimating above-ground biomass and carbon stocks. However, achieving higher accuracy in FCH prediction remains challenging and requires further investigation. Integrating additional datasets, such as data from the recently launched ESA Biomass mission or ICESat-2 observations, to expand point sample coverage, could further improve FCH estimation accuracy in future studies.

Acknowledgement

This paper was developed as part of the TANZEO-BioStock project. The authors acknowledge the support provided by the European Space Agency (ESA) through the EO Africa R&D Facility. *Soheil Zaghian* and *Seyed Ehsan Khankeshizadeh* also gratefully acknowledge the Erasmus+ ICM student mobility programme for supporting a research stay at the Department of Technology and Society, LTH, Lund University, Sweden.

References

Alvites, C., O’Sullivan, H., Francini, S., Marchetti, M., Santopuoli, G., Chirici, G., Lasserre, B., Marignani, M., & Bazzato, E. (2024). High-Resolution Canopy Height Mapping: Integrating NASA’s Global Ecosystem Dynamics Investigation (GEDI) with Multi-Source Remote Sensing Data. *Remote Sensing*, *16*(7), 1281. https://doi.org/10.3390/rs16071281

Asner, G., & Martin, R. (2008). Spectral and chemical analysis of tropical forests: Scaling from leaf to canopy levels. *Remote Sensing of Environment*, *112*(10), 3958–3970. https://doi.org/10.1016/j.rse.2008.07.003

Bruggisser, M., Dorigo, W., Dostálová, A., Hollaus, M., Navacchi, C., Schlaffer, S., & Pfeifer, N. (2021). Potential of Sentinel-1 C-Band Time Series to Derive Structural Parameters of Temperate Deciduous Forests. *Remote Sensing*, *13*(4), 798. https://doi.org/10.3390/rs13040798

Cagnina, C., Marino, A., Silva-Perez, C., Ruiz-Ramos, J., & Suarez, J. (2023). Assessment of the Impact of Surface Water Content for Temperate Forests in SAR Data at C-Band. *Remote Sensing*, *15*(24), 5723. https://doi.org/10.3390/rs15245723

Chen, M., Dong, W., Yu, H., Woodhouse, I. H., Ryan, C. M., Liu, H., Georgiou, S., & Mitchard, E. T. A. (2025). Multimodal deep learning enables forest height mapping from patchy spaceborne LiDAR using SAR and passive optical satellite data. *International Journal of Applied Earth Observation and Geoinformation*, *143*, 104814. https://doi.org/10.1016/j.jag.2025.104814

Chou, T.-C., Zhu, X., & Reef, R. (2024). Pre- and post-fire forest canopy height mapping in Southeast Australia through the integration of multi-temporal GEDI data, satellite images,

and Convolution Neural Network. International Journal of Remote Sensing, 45(10), 3310–3331. https://doi.org/10.1080/01431161.2024.2343429

Farr, T. G., Rosen, P. A., Caro, E., Crippen, R., Duren, R., Hensley, S., Kobrick, M., Paller, M., Rodriguez, E., Roth, L., Seal, D., Shaffer, S., Shimada, J., Umland, J., Werner, M., Oskin, M., Burbank, D., & Alsdorf, D. (2007). The Shuttle Radar Topography Mission. *Reviews of Geophysics*, *45*(2). https://doi.org/10.1029/2005RG000183

Ghorbanian, A., Zaghian, S., Ahmadi, S. A., Mohammadzadeh, A., & Jamali, S. (2025). Time series of Sentinel-1 and Sentinel-2 imagery for parcel-based crop-type classification using Random Forest algorithm and Google Earth Engine. In *Google Earth Engine and Artificial Intelligence for Earth Observation* (pp. 303–319). Elsevier. https://doi.org/10.1016/B978-0-443-27372-8.00008-8

Hancock, S., McGrath, C., Lowe, C., Davenport, I., & Woodhouse, I. (2021). Requirements for a global lidar system: spaceborne lidar with wall-to-wall coverage. *Royal Society Open Science*, *8*(12). https://doi.org/10.1098/rsos.211166

Lang, N., Jetz, W., Schindler, K., & Wegner, J. D. (2023). A high-resolution canopy height model of the Earth. *Nature Ecology & Evolution*, *7*(11), 1778–1789. https://doi.org/10.1038/s41559-023-02206-6

Lei, Y., Wang, Y., Wang, G., Song, C., Cao, H., & Xiao, W. (2024). Estimating Forest Canopy Height based on GEDI Lidar Data and Multi-source Remote Sensing Images. *The International Archives of the Photogrammetry, Remote Sensing and Spatial Information Sciences*, *XLVIII-1–2024*, 297–303. https://doi.org/10.5194/isprs-archives-XLVIII-1-2024-297-2024

Li, X., Wessels, K., Armston, J., Hancock, S., Mathieu, R., Main, R., Naidoo, L., Erasmus, B., & Scholes, R. (2023). First validation of GEDI canopy heights in African savannas. *Remote Sensing of Environment*, *285*, 113402. https://doi.org/10.1016/j.rse.2022.113402

Li, Y., Fang, H., Wang, Y., Li, S., Ma, T., Wu, Y., & Tang, H. (2024). Validation of the vertical canopy cover profile products derived from GEDI over selected forest sites. *Science of Remote Sensing*, *10*, 100158. https://doi.org/10.1016/j.srs.2024.100158

Li, Y., Lu, D., Lu, Y., & Li, G. (2024). Examining the Impact of Topography and Vegetation on Existing Forest Canopy Height Products from ICESat-2 ATLAS/GEDI Data. Remote Sensing, 16(19), 3650. https://doi.org/10.3390/rs16193650

Mauya, E. W., & Madundo, S. (2021). Aboveground biomass and carbon stock of Usambara tropical rainforests in Tanzania. *Tanzania Journal of Forestry and Nature Conservation*, *90*(2), 63–82.

Pirotti, F., Adedipe, O., & Leblon, B. (2023). Sentinel-1 Response to Canopy Moisture in Mediterranean Forests before and after Fire Events. *Remote Sensing*, *15*(3), 823. https://doi.org/10.3390/rs15030823

Pourshamsi, M., Xia, J., Yokoya, N., Garcia, M., Lavalle, M., Pottier, E., & Balzter, H. (2021). Tropical forest canopy height estimation from combined polarimetric SAR and LiDAR using machine learning. ISPRS Journal of Photogrammetry and Remote Sensing, 172, 79–94. https://doi.org/10.1016/j.isprsjprs.2020.11.008

Rajab Pourrahmati, M., Baghdadi, N., & Fayad, I. (2023). Comparison of GEDI LiDAR Data Capability for Forest Canopy Height Estimation over Broadleaf and Needleleaf Forests. *Remote Sensing*, *15*(6), 1522. https://doi.org/10.3390/rs15061522